Journal of Ultrafine Grained and Nanostructured Materials
https://jufgnsm.ut.ac.ir
Vol. 51, No.1, June 2018, pp. 77-83
Print ISSN: 2423-6845 Online ISSN: 2423-6837
DOI: 10.22059/JUFGNSM.2018.01.10

Sol-gel Synthesis of (Ca-Ba)TiO_3 Nanoparticles for Bone Tissue Engineering

Narges Ahmadi Khoei, Mahshid Kharaziha* , Sheyda Labbaf

Department of Materials Engineering, Isfahan University of Technology, Isfahan, Iran.

Recieved: 24 January 2018; Accepted: 15 April 2018

** Corresponding author email: kharaziha@cc.iut.ac.ir*

ABSTRACT

Piezoelectric materials are the group of smart materials which have been recently developed for biomedical applications, such as bone tissue engineering. These materials could provide electrical signals with no external source power making them effective for bone remodeling. Between various types of materials, $BaTiO_3$ and $CaTiO_3$ are nontoxic piezoelectric ceramics, which recently have been introduced for bone tissue engineering. It is expected that, the combination of these two ceramics could provide suitable piezoelectricity, bioactivity and biocompatibility for bone tissue engineering applications. The aim of this research is to synthesize $(Ba_xCa_{1-x})TiO_3$ (x= 0, 0.6, 0.8, 0.9 and 1) nanopowder using sol-gel method. Moreover, the incorporation of Ca^{+2} ions in the structure of $(Ba_xCa_{1-x})TiO_3$ nanoparticles was chemically, structurally and biologically studied. X-ray diffraction (XRD) and scanning electron microscopy (SEM) studies confirmed the role of substituted Ca content on the chemical properties and morphology of particles. Indeed, increasing the amounts of Ca^{+2} ions resulted in the reduced crystallite size. While incorporation of more than 20 at.% Ca resulted in the formation of a biphasic structure, monophasic solid solution without any secondary phase was detected at less Ca content. Moreover, SEM images revealed that Ca substitution reduced particle size from 70.5 ±12 nm to 52.4 ±9 nm, while the morphology of synthesized powders did not significacntly change. Furthermore, incorporation of upon 10 at.% Ca content within $(Ba_xCa_{1-x})TiO_3$ significantly promoted MG63 proliferation compared to pure $CaTiO_3$.

Keywords: *Piezoelectric, Bone tissue engineering, $BaTiO_3$; $CaTiO_3$, Sol-gel.*

1. Introduction

Piezoelectric materials are the group of smart materials which can produce a voltage by applying mechanical stress or vice-versa [1]. Different natural and synthetic piezoelectric ceramics (e.g. calcium titanate, barium titanate and lead zirconate titanate (PZT) [2]) and polymers (e.g. PVDF) [1] have been introduced for various applications. Ability of electrical ceramics for applying in biomaterials region particularly with piezoelectric properties was indicated in recent years [3]. Function of specific cells from the aspect of adhesion, proliferation and differentiation can be improved by application of smart materials like piezoelectric groups in tissue engineering [4]. Indeed, the use of the active materials for this area (for example as scaffold) could provide the necessary stimuli for proper tissue regeneration. In addition to the synthetic materials, many body tissues are piezoelectric like bone, cartilage, DNA, tendons and etc. [5]. Between them, bone is a dynamic tissue with very low piezoelectric coefficient (0.7 pC/N) which its piezoelectric nature was reported by Yasuda in 1954 (6). This tissue can response to micromechanical stresses like the movement of the body and leads to produce electrical dipole

and signals which can improve bone growth and remodeling according to the Wolff's law [5, 7]. In addition, electrical signals can instigate the osteogenic activities which is beneficial for bone healing [1]. Therefore, utilization of piezoelectric materials for bone tissue engineering can be a promising technique for reconstruction of bone defects [6]. These materials can be used as charge provider agent for stimulating bone implant healing process [3]. Because of the presence of toxic lead in its structure, PZT is not common in bone tissue engineering, despite its high piezoelectric coefficient [6].

Barium titanate is the first and the most studied lead free piezo-ceramic applied for bone repair [6, 7]. Recently, promising results reported that a strong interfacial bond was observed between barium titanate cylinders implanted in canine femora with bone. Moreover, in vivo studies showed faster new bone formation on the barium titanate/hydroxyapatite than pure hydroxyapatite one [6]. On the other hand, calcium titanate is another piezoelectric ceramic which has been applied for biomedical applications in various forms (powder, coating and foam) [8,9]. Recent results confirmed that calcium titanate coatings on titanium promoted osteoblast adhesion compared to uncoated titanium implants [8]. Bagchi et al. [9] developed nanocomposite of poly (ε-caprolactone) (PCL) with different perovskite nanoparticles including calcium titanate (CT), barium titanate (BT) and strontium titanate (ST) for bone tissue engineering. In vitro studies revealed the enhanced osteogenic genes on PCL/CT nanocomposites compared to other composites. However, results showed that the piezoelectric properties of calcium titanate are weaker than barium titanate [9]. Substituting calcium in barium titanate structure can make $(Ba_xCa_{1-x})TiO_3$ (BCT) crystals a promising candidate for lead free piezoelectric materials [10]. Zhuang et al. [11] report the possibility of Ca^{2+} occupation in $BaTiO_3$ structure, for the first time. Following this report, different processing routes have been applied for Ca^{2+} substitution in $BaTiO_3$ structure [11]. Conventionally, $(Ba,Ca)TiO_3$ powder is synthesized by solid-state reaction between a mixture of TiO_2, $BaCO_3$ and $CaCO_3$. However, obtained powders often consist of coarse grains with non-uniform particle size and shape [12]. In addition, $(Ba, Ca)TiO_3$ powder synthesized via solid-state reaction consists of low solubility limit of Ca^{2+} [12]. Nowadays, wet chemical processes are a preferred way of synthesis due to high solubility limit, stoichiometry control, reproducibility, purity and small particle size of products[12]. These wet chemical techniques consist of carbonate-oxalate [11], gel-carbonate [11], gel-to-crystallite conversion [11], hydrothermal [13], sol-gel [14] and polymeric precursor [15] approach. Amongst them, sol-gel process enables a better control of size and morphology with least impurity [16]. Li et al [14] synthesized $(Ba_{0.9}Ca_{0.1})TiO_3$ powder with grain size of 2 μm using sol-gel process. However, the role of various concentrations of substituted Ca on the properties of $(Ba_xCa_{(1-x)})TiO_3$ was not investigated. It was expected that incorporation of calcium ions within barium titanate could stimulatory promote both piezoelectric and biological properties. So, the aim of this study was to synthesize $(Ba_xCa_{1-x})TiO_3$ (x= 0, 0.6, 0.8, 0.9 and 1) nanopowders by a simple sol-gel method. Moreover, the effects of Ca^{2+} substitution on the chemical and biological properties of barium titanate were investigated.

2. Experimental

2.1. Materials

Glacial acetic acid (assay 100 %), calcium nitrate tetrahydrate (assay 99 %), barium acetate, titanium tetraisopropyl alkoxide (TTIP, assay 98 %) and 2-propanol (assay >99 %) were purchased from Merck company.

2.2. Synthesis of barium-calcium titanate powders

In order to synthesize $(Ba_xCa_{1-x})TiO_3$ (x= 0, 0.6, 0.8, 0.9 and 1), barium acetate and calcium nitrate were used as barium and calcium precursors. In this regard, calcium nitrate tetrahydrate and barium acetate were dissolved in acetic acid at 65 °C, separately. In the next step, both solutions were cooled down to room temperature for adding 2-propanol and TTIP, respectively. The above precursors were selected in order to provide sols with acetic acid: TTIP:2-propanol: deionized water molar ratio=6:1:1:150. After mixing two solutions, the temperature was reached to 2-3 °C and deionized water was incorporated to the solution to form a transparent sol. After forming gel via hotplate at 60°C, it was dried at 100 °C for 24 h. As prepared dried gels were ball milled with speed of 250 rpm for 1 h and finally were calcined at 1000 °C for 2 h to obtain white powders. Based on the amount of Ca content, samples were named as BT, BCT1, BCT2, BCT3 and CT referred to $BaTiO_3$,

$(Ba_{0.9}Ca_{0.1})TiO_3$, $(Ba_{0.8}Ca_{0.2})TiO_3$, $(Ba_{0.6}Ca_{0.4})TiO_3$ and $CaTiO_3$ samples, respectively.

2.3. Characterization of barium-calcium titanate powders

The crystal structure and phase analysis of prepared powders was performed using the X-ray Diffraction (XRD, Philips X'Pert-MPD, Holland) with Cu Kα radiation (λ=0.542) and time per step 1.25 sec. Results were analyzed by X'Pert High Score software. The surface morphology of powders was characterized using Scannig Electron Microscopy (SEM, Philips XL30 SERIES) and average particle size was characterized with ImageJ software.

The cytotoxicity assay was evaluated using a dilution of nanopowder with various concentrations in contact with MG63 cells according to the International Standard Organization (ISO/EN 10993.5, 1999). Briefly, MG63 cell lines were exposed to a series of nanopowder extracts in the full culture medium. Prior to cell culture, the 200 μg/ml of calcium-barium titanate powders were prepared in complete culture medium. After 24 h incubation at 37 °C, the mixtures were diluted further to provide powder extracts with various concentrations of 50 and 100 μg/ml. MG63 cells were seeded at density of 10^4 cells/well in a 96-well plate. After 24 h incubation, the medium was removed and replaced with diluted extracts (50, 100 and 200 μg/ml).

The relative viability of cells was studied by 3-(4,5-dimethylthiazolyl-2)-2,5-diphenyl tetrazolium bromide (MTT, Sigma-Aldrich) colorimetric assay. After one day of culture, the medium was discarded, the wells were washed with PBS and the samples were incubated with MTT solution (0.5 mg/ml MTT reagent in PBS) for 4 h. As formed dark blue formazan crystals were dissolved with dimethyl sulfoxide (DMSO, Sigma) and kept for 30 min at 37 °C. Subsequently, the optical density (OD) of each well was measured with a microplate reader (Bio Rad, Model 680 Instruments) against DMSO (blank) at a wavelength of 490 nm.

3. Results and Discussion

The chemical structure of the powders was studied using XRD technique. To determine phase compositions, the patterns were matched to the Joint Committee on Powder Diffraction Standards (JCPDS) reference files. Figure 1 shows XRD patterns of $(Ba_xCa_{1-x})TiO_3$ powders consisting of various mounts of Ca content (BT, BCT1, BCT2, BCT3, CT). Results showed that XRD patterns of $BaTiO_3$ (BT) and $CaTiO_3$ (CT) only consisted of the characteristic peaks of pure barium titanate and calcium titanate, respectively, without any new peak confirming the formation of pure BT and CT powders. The BT and CT lattice parameters were in agreement with the reported data (reference code: JCPDS 01-079-2263 and JCPDS 01-081-0561, respectively). Between various $(Ba_xCa_{1-x})TiO_3$ powders, $(Ba_{0.9}Ca_{0.1})TiO_3$ (BCT1) and $(Ba_{0.8}Ca_{0.2})TiO_3$ (BCT2) revealed only the characteristic peaks of BT (reference code: JCPDS 00-008-0725) confirming the formation of solid solution monophase without any secondary phase. Previous researches also confirmed that pure barium titanate could be formed when x ≤23% (BT , BCT1 and BCT2 samples) [10]. When x reached to 40% (BCT3($(Ba_{0.6}Ca_{0.4})TiO_3$)), biphasic structure of BT and CT was developed showing the imperfect homogeneity due to incomplete diffusion of Ca into $BaTiO_3$ [10].

In addition to phase composition, the crystal structure of barium titanate changed with incorporation of Ca within the structure. Table 1 shows the crystallographic structure of different BCT powders consisting of various amounts of Ca content. According to JCPDS reference files, BCT1 and BCT2 samples showed the crystal structure of tetragonal. With increasing the Ca content in BCT3 sample, crystal structure of barium titanate changed into the cubic form. To confirm these results, Rietveld analysis was performed using a MAUD (material analysis using diffraction) software package for considering the crystal structure more precisely. In this way, $(Ba_xCa_{1-x})TiO_3$ (BCT) structure was indexed using tetragonal $BaTiO_3$ (reference code: JCPDS 00-008-0725) for x < 20% (BCT1 and BCT2 samples) and cubic $BaTiO_3$ (reference code: JCPDS 01-079-2263) for BCT3 powders, respectively. Results revealed that the lattice volume enhanced in BCT1 sample confirming the substituting Ti^{4+} by Ca^{2+} ions. Moreover, c/a ratio enhanced at BCT1 sample demonstrating its tetragonal structure. Our results revealed that substituting 10 at.% Ca ions resulted in changing the crystallographic structure of $BaTiO_3$ from cubic to tetragonal. More Ca substitution for Ba in BCT2 and BCT3 samples led to reduce in its volume structure and tetragonality (c/a). This behavior was similarly reported in previous researches [17]. In the case of BCT3 sample, the crystallographic structure changed to cubic one.

These changes might be due to the substitution of smaller Ca $^{2+}$ for larger Ba^{2+} leading to shrinkage of crystal structure.

Moreover, the crystallite size of all synthesized samples was calculated from XRD pattern with standard data compiled by the International Center for Diffraction Data (ICDD) using the modified Scherrer formula (eq. 1) [18]:

$$ln\,\beta = ln\,\frac{k\,\lambda}{L} + ln\,\frac{1}{\cos\theta} \qquad \text{(eq. 1)}$$

where L is the crystallite size (nm), λ is the wavelength of Cu kα radiation (λ= 1.5404 °A), β is the full width at half maximum (FWHM) for the diffraction peak under consideration (in radian), θ is the diffraction angle (°) and k is the broadening constant. The crystallite size of synthesized powders are presented in Table 1. Results confirmed that CT samples revealed the smallest crystallite size (16 nm) between various samples. Moreover, substitution of Ca^{+2} ions for Ba^{2+} in BT structure reduced the crystallite size of powder from 35 nm (at BT powder) to 28 nm (at BCT3). This result was similarly reported in previous researches in which $(Ba_xCa_{1-x})TiO_3$ was synthesize using other techniques [19, 20].This reduction with increasing Ca content might be due to the substitution of smaller Ca $^{2+}$ to larger Ba^{2+} leading to shrinkage of crystal structure [21].

The morphology of $(Ba_xCa_{1-x})TiO_3$ nanopowders was investigated by SEM (Figure 2) and the average particle sizes of the synthesized powders was

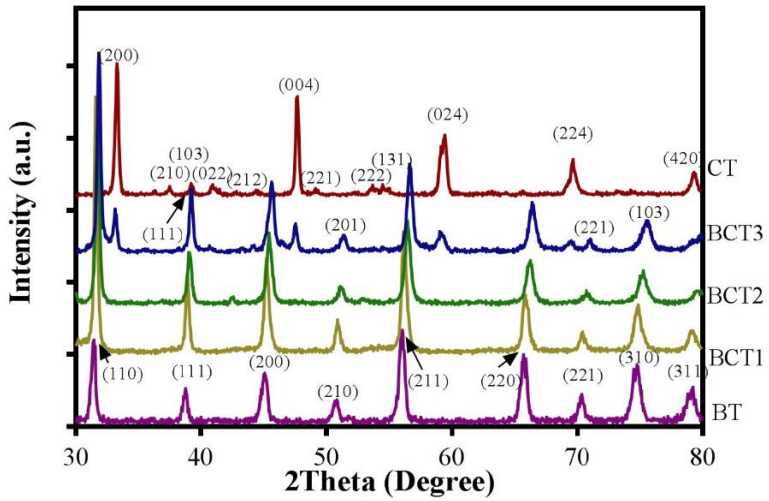

Fig. 1- XRD patterns of $(Ba_xCa_{1-x})TiO_3$ powders.

Table 1- The crystallographic structure and crystallite size of $(Ba_xCa_{1-x})TiO_3$ obtained from XRD patterns

Sample code	Structure	Crystallite size(nm)
BT($BaTiO_3$)	Cubic	35
BCT1((0.9Ba:0.1Ca)TiO_3)	Tetragonal($BaTiO_3$)	35
BCT2((0.8Ba:0.2Ca)TiO_3)	Tetragonal($BaTiO_3$)	34
BCT3((0.6Ba:0.4Ca)	Cubic($BaTiO_3$)	
TiO_3)	Orthorhombic($CaTiO_3$)	28($BaTiO_3$)
CT($CaTiO_3$)	Orthorhombic	16

estimated using Image J software and are presented in Table 2. Results revealed that Ca substitution did not alter the spherical morphology of the synthesized powders. However, the average particle size of powders was reduced, depending on the calcium content incorporated into the structure. It

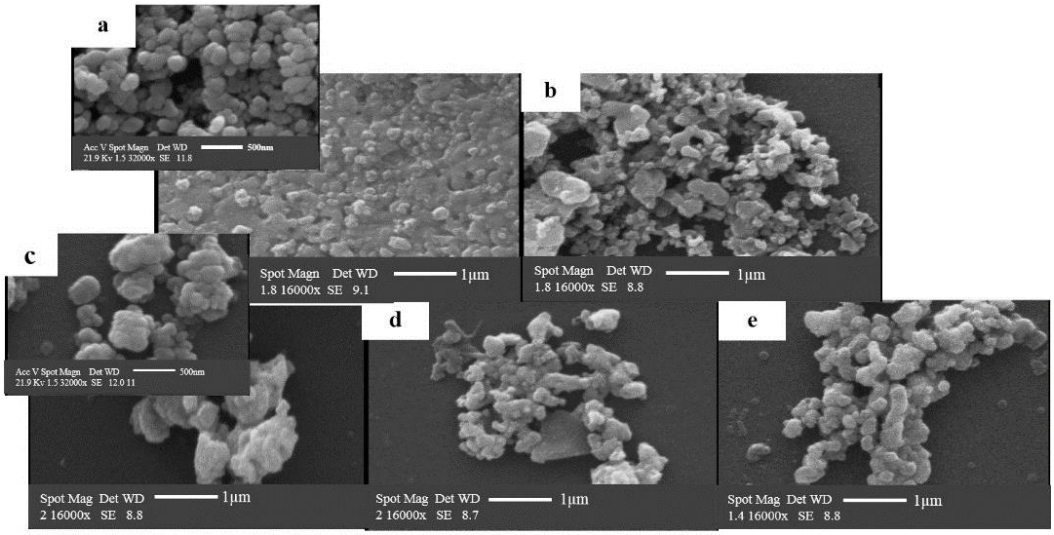

Fig. 2- SEM images of BT (a), CT(b), BCT1(c), BCT2(d) and BCT3(e) at 16000× magnification.

Table 2- Morphology and particle size of $(Ba_xCa_{1-x})TiO_3$ extracted from SEM images

Sample code	Morphology	Particle size(nm)
BT	Spherical	70.5±12
BCT1(0.9Ba:0.1Ca)	Spherical	68 ±12
BCT2(0.8Ba:0.2Ca)	Spherical	65±19
BCT3(0.6Ba:0.4Ca)	Spherical	52.4±9.3
CT(0Ba:1Ca)	Spherical	54.4±13.3

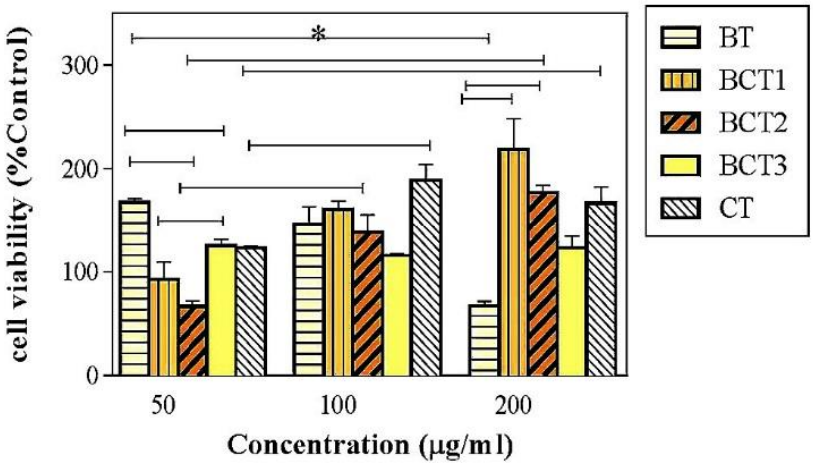

Fig. 3- Viability of MG63 cells cultured on various $(Ba_xCa_{1-x})TiO_3$ samples using MTT assays after 1 day of culture (* P<0.05).

was suggested that the reduced particle size detected as a result of increased Ca content could be due to the substitution of smaller Ca $^{2+}$ for a larger Ba^{2+} leading to the shrinkage of crystal structure and/or due to the role of Ca ions in inhabitation of the grain growth during calcification [21].

The cytotoxicity of various samples on MG63 cells cultured for 1 day was determined by MTT assay (Figure 3). The relative cell survival was calculated based on the following equation (eq. 2):

$$\text{Relative cell survival (\%)} = \frac{A_{sample} - A_b}{A_{control} - A_b} \qquad \text{(eq. 2)}$$

where A_{sample}, A_b and $A_{control}$ are the absorbance of sample, blank (DMSO) and control (TCP), respectively.

Results demonstrated that the proliferation of MG63 cells cultured on BCT1, BCT2 and CT samples gradually enhanced from at least concentration (50 µg/ml) to the highest concentrations (200 µg/ml), while various concentrations of BCT3 did not significantly change it. Noticeably, the viability of cells enhanced from 92.7±12 %control (at 50 µg/ml of BCT1) to 218.8±21 %control (at 200 µl/ml of BCT1)($P<0.05$). Moreover, increasing the concentrations of BT sample dramatically reduced the viability of MG63 cells ($P<0.05$). According to the results, between various samples at different concentrations of 50, 100 and 200 µg / ml, BCT1 samples provided the best condition for cell viability. Our results showed that the replacement of calcium ions in the structure of barium titanate not only did not reveal any cytotocxic behavior, but also could significantly improve in the case of BCT1.

4. Conclusions

In this study, barium calcium titanate with various Ca contents (0, 0.1, 0.2, 0.6 and 1 at.%) were successfully synthesized by sol–gel method. Moreover, the effects of Ca concentration on the structural and chemical properties of nanopowder were investigated. XRD patterns confirmed the successfully substitution of Ca^{+2} ions within the structure which resulted in changing the crystallographic structure from cubic symmetry to tetragonal. Moreover, incorporation of Ca ions within the barium titanate structure led to decrease in average crystallite (from 35 nm to 28 nm) and particle size (from 70.5±12 nm to 52.4±9.3 nm). Fz of Ca ions within the barium titanate powder upon 10% significantly promoted MG63 proliferation compared to pure barium titanate and calcium titanate, which might be due to the effective role of calcium to improve cell behavior. These results suggested that barium calcium titanate could be an excellent potential candidate for bone tissue engineering applications.

References

1. Ribeiro C, Sencadas V, Correia DM, Lanceros-Méndez S. Piezoelectric polymers as biomaterials for tissue engineering applications. Colloids and Surfaces B: Biointerfaces. 2015;136:46-55.
2. Press Llc C. The Measurement, Instrumentation and Sensors Handbook on CD-ROM: CRC Press; 1999 1999/02/26.
3. Zanfir AV, Voicu G, Jinga SI, Vasile E, Ionita V. Low-temperature synthesis of BaTiO 3 nanopowders. Ceramics International. 2016;42(1):1672-8.
4. Ribeiro C, Pärssinen J, Sencadas V, Correia V, Miettinen S, Hytönen VP, et al. Dynamic piezoelectric stimulation enhances osteogenic differentiation of human adipose stem cells. Journal of Biomedical Materials Research Part A. 2014;103(6):2172-5.
5. Ribeiro C, Sencadas V, Correia DM, Lanceros-Méndez S. Piezoelectric polymers as biomaterials for tissue engineering applications. Colloids and Surfaces B: Biointerfaces. 2015;136:46-55.
6. Rajabi AH, Jaffe M, Arinzeh TL. Piezoelectric materials for tissue regeneration: A review. Acta Biomaterialia. 2015;24:12-23.
7. Zhang Y, Chen L, Zeng J, Zhou K, Zhang D. Aligned porous barium titanate/hydroxyapatite composites with high piezoelectric coefficients for bone tissue engineering. Materials Science and Engineering: C. 2014;39:143-9.
8. Thuy Ba Linh N, Mondal D, Lee BT. In Vitro Study of CaTiO3–Hydroxyapatite Composites for Bone Tissue Engineering. ASAIO Journal. 2014;60(6):722-9.
9. Bagchi A, Meka SRK, Rao BN, Chatterjee K. Perovskite ceramic nanoparticles in polymer composites for augmenting bone tissue regeneration. Nanotechnology. 2014;25(48):485101.
10. Purwanto A, Hidayat D, Terashi Y, Okuyama K. Synthesis of Monophasic CaxBa(1–x)TiO3Nanoparticles with High Ca Content (x> 23%) and Their Photoluminescence Properties. Chemistry of Materials. 2008;20(24):7440-6.
11. Jayanthi S, Kutty TRN. Extended phase homogeneity and electrical properties of barium calcium titanate prepared by the wet chemical methods. Materials Science and Engineering: B. 2004;110(2):202-
12. Zhang W, Shen Z, Chen J. Preparation and characterization of nanosized barium calcium titanate crystallites by low temperature direct synthesis. Journal of materials science. 2006 Sep 1;41(17):5743-5.
13. Tikhonovsky A, Kim K, Lee SK, Nedoseykina T, Yang M, Song SA. Effect of Ca addition on Grain Size and Crystal Phase of Barium Titanate Nanopowders. Japanese Journal of Applied Physics. 2006;45(10A):8014-9.
14. Li L-Y, Tang X-G. Effect of electric field on the dielectric properties and ferroelectric phase transition of sol–gel derived (Ba0.90Ca0.10)TiO3 ceramics. Materials Chemistry and Physics. 2009;115(2-3):507-11.
15. da Silva RS, Bernardi MIB, Hernandes AC. Synthesis of non-agglomerated Ba0.77Ca0.23TiO3 nanopowders by a modified polymeric precursor method. Journal of Sol-Gel Science and Technology. 2007;42(2):173-9.
16. Ji B, Chen D, Jiao X, Zhao Z, Jiao Y. Preparation and electrical properties of nanoporous BaTiO3. Materials Letters. 2010;64(16):1836-8.
17. Singh B, Kumar S, Arya GS, Negi NS. Room temperature structural and electrical properties of barium calcium titanate (BCT) thin films. AIP Publishing LLC; 2015.

18. Monshi A, Foroughi MR, Monshi MR. Modified Scherrer Equation to Estimate More Accurately Nano-Crystallite Size Using XRD. World Journal of Nano Science and Engineering. 2012;02(03):154-60.
19. Souza AE, Silva RA, Santos GTA, Moreira ML, Volanti DP, Teixeira SR, et al. Photoluminescence of barium–calcium titanates obtained by the microwave-assisted hydrothermal method (MAH). Chemical Physics Letters. 2010;488(1-3):54-6.
20. Mitsui T, Westphal WB. Dielectric and X-Ray Studies ofCaxBa1−xTiO3andCaxSr1−xTiO3. Physical Review. 1961;124(5):1354-9.
21. Matsuura K, Hoshina T, Takeda H, Sakabe Y, Tsurumi T. Effects of Ca substitution on room temperature resistivity of donor-doped barium titanate based PTCR ceramics. Journal of the Ceramic Society of Japan. 2014;122(1426):402-5.